DALTON

pH-Dependent competition between $\kappa^2N^7,O(P)$ macrochelation and μ-N^1,N^7 oligomer formation for (η^6-arene)Ru^{II} complexes of adenosine and guanosine 5′-mono-, -di- and -tri-phosphates

Sandra Korn and William S. Sheldrick*

Lehrstuhl für Analytische Chemie, Ruhr-Universität Bochum, D-44780 Bochum, Germany

The pH-dependent reaction of $[Ru(\eta^6\text{-}C_6H_6)(D_2O)_3]^{2+}$ with adenosine and guanosine 5′-mono-, -di- and -tri-phosphates has been studied by ^1H and $^{31}P\text{-}\{^1H\}$ NMR spectroscopy. Diastereomeric $\mu\text{-}1\kappa N^1:2\kappa^2N^6$, N^7 co-ordinated cyclic trimers of the type $[\{Ru(5'\text{-}AMP)(\eta^6\text{-}C_6H_6)\}_3]$ predominate for adenosine 5′-monophosphate ($5'\text{-}AMP^{2-}$) in the range pH* 3.30–9.18. An X-ray structural analysis of the $Ru_SRu_SRu_S$ diastereomer $[\{Ru(5'\text{-}AMP)(\eta^6\text{-}p\text{-}MeC_6H_4Pr^i)\}_3]\cdot 7.5H_2O$ **1b** established a pronounced degree of conformational flexibility in the sugar and phosphate residues. In contrast to $5'\text{-}AMP^{2-}$, cyclic trimers cannot be observed in more strongly acid solution (pH* ≤ 3.16) for the equilibrium system 5′-ATP–(η^6-C_6H_6)Ru^{II} ($5'\text{-}ATP^{4-}$ = adenosine 5′-triphosphate) and remain relatively minor species even at neutral or higher pH* values. As confirmed by pronounced low-field $^{31}P\text{-}\{^1H\}$ NMR shifts of up to 7.8 and 8.6 ppm for the β- and γ-phosphorus atoms, κ^3N^7, $O(P_\beta)$, $O(P_\gamma)$ macrochelates provide the dominant metal species in acid solution. Time-dependent NMR studies for 5′-ADP–(η^6-C_6H_6)Ru^{II} ($5'\text{-}ADP^{3-}$ = adenosine 5′-diphosphate) indicated that initial macrochelation of this nucleotide is followed by cleavage of the β-phosphate group and formation of cyclic trimers of $5'\text{-}AMP^{2-}$. Reaction of guanosine 5′-monophosphate ($5'\text{-}GMP^{2-}$) with $[Ru(\eta^6\text{-}C_6H_6)(D_2O)_3]^{2+}$ afforded κN^7-co-ordinated 1:1 and 2:1 complexes in the range pH* 3.69–8.38. In addition to analogous 1:1 and 2:1 species, κ^3N^7, $O(P_\beta)$, $O(P_\gamma)$ macrochelates are observed for the 5′-GTP–(η^6-C_6H_6)Ru^{II} equilibrium system ($5'\text{-}GTP^{4-}$ = guanosine 5′-triphosphate) in acid solution. Initial macrochelation in the 5′-GDP–(η^6-C_6H_6)Ru^{II} system ($5'\text{-}GDP^{3-}$ = guanosine 5′-diphosphate) again leads to rapid cleavage of the terminal β-phosphate function.

The presence of metal ions such as Mg^{2+} is generally a prerequisite for enzymatic reactions involving nucleotides. Both hard oxygen atoms in the phosphate and sugar moieties and borderline aromatic nitrogen atoms in the purine or pyrimidine residues are available as potential binding sites in these structurally flexible bioligands.[1–3] Differences in the basicities of the endocyclic base nitrogen sites have been demonstrated to be of crucial importance for the selective recognition of metal ions by nucleic acids and their constituents.[4] For instance, it is well known[5] that the widely used antitumour agent *cis*-$[PtCl_2(NH_3)_2]$ preferably binds to the guanine and not the adenine bases of DNA. For borderline metal ions such as Fe^{2+}, Cu^{2+} or Zn^{2+} with their rather pronounced affinity for aromatic nitrogen sites, significant binding to the phosphate oxygen atoms might also be expected. Such a simultaneous interaction with two component parts of a nucleotide could provide a further degree of fine tuning for the selective recognition of metal ions.

The possibility of macrochelate formation by purine nucleotides through co-ordination of a metal centre by both the nucleic base and phosphate residues was first discussed by Szent-Györgyi[6] in 1956. Despite continuous interest in this suggestion, 30 years were to pass before definitive kinetic and spectroscopic confirmation of simultaneous direct metal binding to both the phosphate group and the purine N^7 atom was presented.[7–10] Mononuclear macrochelates of the type $[ML_x\{5'\text{-}NMP\text{-}\kappa^2N^7,O(P_\alpha)\}]^{n+}$ have now been established by NMR investigations for the *cis*-$(CH_3ND_2)_2Pt^{II}$,[7a,b] $Cl(dmso)_2(H_2O)Ru^{II}$ (dmso = dimethyl sulfoxide),[7c] $(H_2O)(tren)Rh^{II}$ [tren = tris(2-aminoethyl)amine][7d] and $(cp)_2Mo^{IV}$ (cp = η^5-C_5H_5)[9] fragments with purine 5′-nucleoside monophosphates (5′-H_2NMP). Fast atom bombardment mass spectrometric and kinetic studies for the product of the reaction between *cis*-$[Pt(H_2O)_2(NH_3)_2]^{2+}$ and $5'\text{-}GMP^{2-}$ or 5′-(2′-deoxy)GMP^{2-} also indicate direct intramolecular co-ordination of both nucleotide residues.[8] The increased stability of various $5'\text{-}NMP^{2-}$ complexes of divalent 3d ions in comparison to expected values for phosphate-only co-ordination demonstrates that macrochelated species must be present in appreciable concentration.[3,4] Support for inner-sphere co-ordination of both the phosphate group and the purine N^7 atom is provided by kinetic studies[11] and modelling considerations.[12]

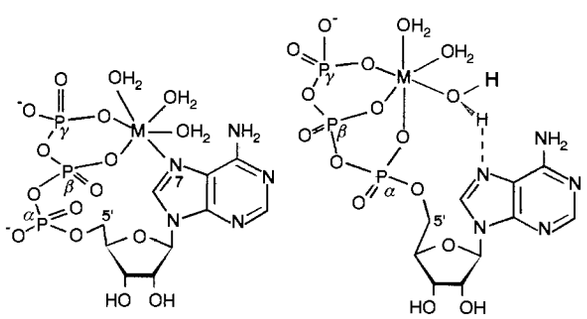

Scheme 1 N^7 Inner- and outer-sphere macrochelates for the reaction between $5'\text{-}ATP^{4-}$ and divalent 3d ions

Purine 5′-nucleoside di- and tri-phosphates ($5'\text{-}NDP^{3-}$, $5'\text{-}NTP^{4-}$) can form α, β- and α, β, γ-phosphate-co-ordinated inner- and outer-sphere macrochelates of the types I and II (Scheme 1 for $5'\text{-}ATP^{4-}$) with divalent 3d ions in aqueous solution. Sigel[3] has estimated the extent of inner-sphere co-ordination by comparing stability constants determined by potentiometric and ultraviolet absorption techniques. The extent of formation of type I complexes is found to vary between *ca.* 10% for Mn^{2+} and 67% for the softer Cu^{2+} cation.

Proton and ^{31}P NMR evidence has been presented by Marzilli and co-workers[7b] that *cis*-$(CH_3ND_2)_2Pt^{II}$ co-ordinates to purine 5′-nucleoside triphosphates in dilute D_2O solution in an intramolecular fashion to both N^7 and a γ-phosphate oxygen atom. These authors also observed the involvement of N^1 in Pt binding at a Pt:$5'\text{-}ATP^{4-}$ ratio greater than one and postulated

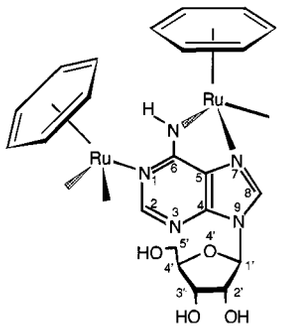

Scheme 2 μ-1κN^1:2κ$^2N^6$,N^7 Bridging[16b] in the cyclic trimer [{Ru(μ-$AdoH_{-1}$)(η^6-C_6H_6)}$_3$]$^{3+}$

the formation of μ-N^1,N^7 bridged oligomers in competition with κ$^2N^7$,$O(P_\gamma)$ macrochelation. Analogous oligomers have been reported for the interaction of the 5′-monophosphates of adenosine, guanosine and inosine with (en)Pd^{II} (en = ethane-1,2-diamine)[13] and Harada and co-workers[14] have proposed that the apposite 5′-GMP^{2-} complex is a cyclic tetramer. On binding to N^7, Pd^{II} enhances the deprotonation of N^1 in guanosine and inosine derivatives[15] with the result that κN^7 co-ordinated 1:2 complexes such as [Pd(5′-HGMP-κN^7)$_2$(en)] exhibit an increased tendency to disproportionate to μ-N^1,N^7 bridged oligomers and unbound 5′-GMP^{2-} on raising the pH value.[13b] The recent characterisation of μ-1κN^7:2κN^9 co-ordinated tetramers such as [{RuCl(μ-HAde)(η^6-C_6H_6)}$_4$]Cl_4 (HAde = adenine)[16a] and μ-1κN^1:2κ$^2N^6$,N^7 co-ordinated trimers (Scheme 2) such as [{Ru(μ-$AdoH_{-1}$)(η^6-C_6H_6)}$_3$][CF_3SO_3]$_3$ (Ado = adenosine)[16b] and [{Rh(η-C_5Me_5)(μ-5′-AMP)}$_3$][17] suggests that the formation of cyclic oligomers may well be typical for the reaction of potentially bi- and tri-dentate fragments of heavier Group 8–10 transition metals with purines and their nucleoside 5′-phosphates.

To our knowledge no systematic investigation of the competition between macrochelation and oligomer formation has previously been reported for the reaction of purine nucleoside 5′-mono-, -di- and -tri-phosphates with borderline or soft metal cations. We now describe a pH-dependent ^{1}H and ^{31}P NMR study of the interaction of the (η^6-arene)Ru^{II} fragment (η^6-arene = C_6H_6 or *p*-cymene) with adenosine and guanosine nucleotides. X-Ray structural studies are presented where appropriate.

Results and Discussion

Selected ^{1}H NMR spectra for the aqueous 5′-AMP–(η^6-C_6H_6)-Ru^{II} equilibrium system (molar ratio $R_{5'\text{-AMP:Ru}}$ = 1.05) at pH* values (pH meter readings uncorrected for deuterium isotope effects) in the range 3.30–9.18 are presented in Fig. 1. A pronounced downfield shift of H^8 accompanied by an opposite shift for H^2 is characteristic for the μ-1κN:2κ$^2N^6$,N^7 co-ordination mode of bridging adenine derivatives in cyclic trimers of the type [{Ru(μ-$AdoH_{-1}$)(η^6-C_6H_6)}$_3$][16b] or [{Rh(η-C_5Me_5)-(μ-5′-AMP)}$_3$].[17] The signal pair 1,1′ [pH* 3.30; δ 7.64, 7.69 (H^2), 8.88, 8.92 (H^8)] may, therefore, be unambiguously assigned to the diastereomeric pair ($Ru_SRu_SRu_S$/$Ru_RRu_RRu_R$) of the trinuclear cation [{Ru(5′-HAMP)(η^6-C_6H_6)}$_3$]$^{3+}$ at pH* values below 5. Following loss of the second nucleoside 5′-phosphate acid protons in the range pH* 5–7, this signal pair will correspond to the neutral cyclic trimer [{Ru(5′-AMP)-(η^6-C_6H_6)}$_3$] in alkaline solution [pH* 9.18; δ 7.66, 7.71 (H^2), 9.05, 9.08 (H^8)]. The presence of a diastereomeric pair in solution also causes a splitting of the benzene proton resonance at higher pH* values [pH* 9.18; δ 6.00, 6.01 (η^6-C_6H_6)]. Diastereomer 1′ clearly dominates in the investigated pH* range. The apparent inversion of the concentration ratio at pH* 5.30 is caused by a partial crystallisation of the dominant isomer from weakly acidic equilibrium solutions (range pH* 4.13–5.84) at the relatively high concentration (0.050 mol l^{-1}) employed for the NMR study. Signals 2 in Fig. 1 correspond to the H^2 and H^8 resonances of free 5′-$HAMP^-$/5′-AMP^{2-}; signal 3 is only observed at higher pH values and belongs to the dinuclear cation [{Ru(η^6-C_6H_6)}$_2$(μ-$OH)_3$]$^+$.[18] At lower pH* values (3.30, 5.30) the ^{31}P NMR spectra of the 5′-AMP–(η^6-C_6H_6)Ru^{II} equilibrium system (R = 1.05) contain several neighbouring resonances in the range (δ 0.5–1.1) typical for the non-co-ordinated adenosine 5′-monophosphate P atom. These signals shift to lower field (δ 4.50–4.67 at pH* 9.18) in the range pH* 4.5–7.5 in accordance with a second deprotonation of the phosphate group at a typical pK_s value of *ca.* 6.[7c] In contrast to NMR studies on the 5′-AMP–(η^5-C_5Me_5)Rh^{III} equilibrium system,[17b] which exhibits a number of ^{31}P resonances (pH* 5.14) with 8–12 ppm downfield shifts reminiscent of N^7/O(P_α) macrochelate formation,[7–10] no evidence could be found for phosphate co-ordination of the (η^6-C_6H_6)Ru^{II} cation even at a 2:1 excess of the organometallic fragment.

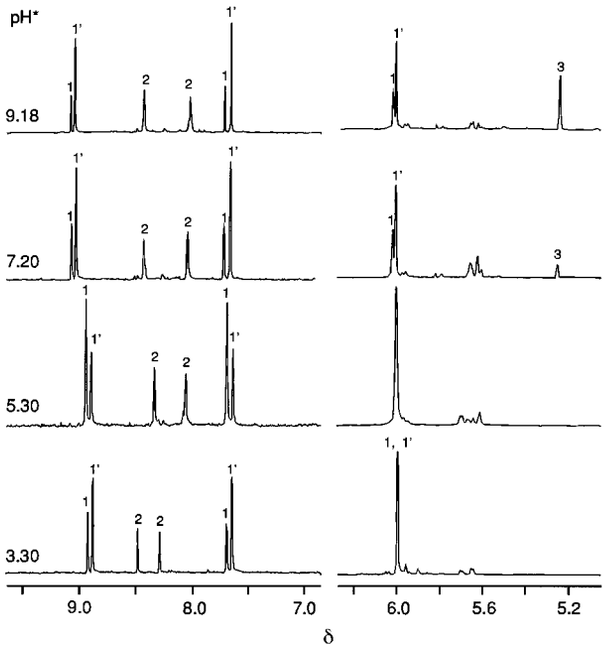

Fig. 1 Selected pH*-dependent ^{1}H NMR spectra for the aqueous equilibrium system 5′-AMP–(η^6-C_6H_6)Ru^{II} at molar ratio $R_{5'\text{-AMP:Ru}}$ = 1.05 (c_{Ru} = 0.050 mol l^{-1}). The signal assignment is as follows: 1,1′, cyclic trimers [{Ru(5′-AMP)(η^6-C_6H_6)}$_3$]; 2,2 5′-AMP^{2-}; 3, [{Ru(η^6-C_6H_6)}$_2$(μ-$OH)_3$]$^+$

The cyclic trimer [{Ru(5′-HAMP)(η^6-*p*-$MeC_6H_4Pr^i$)}$_3$]-[CF_3SO_3]$_3$ **1a** can be prepared by reaction of [Ru(η^6-*p*-$MeC_6H_4Pr^i$)(Me_2CO)$_3$]$^{2+}$ with 5′-H_2AMP in acetone at room temperature. Confirmation of the trimeric structure is provided by the FAB mass spectrum of **1a**, which contains a molecular ion [M − 2CF_3SO_3]$^+$ at *m/z* 1892. Slow evaporation of an aqueous solution of **1a** provided crystals of [{Ru(5′-AMP)-(η^6-*p*-$MeC_6H_4Pr^i$)}$_3$]·7.5H_2O **1b** suitable for an X-ray structural analysis (Fig. 2). The asymmetric unit of **1b** can contain up to 7.5 water molecules distributed over 11 possible sites. As depicted in Fig. 3, the cyclic trimer of the 5′-AMP^{2-} dianion, which crystallises as the $Ru_SRu_SRu_S$ diastereomer, exhibits a pronounced degree of conformational flexibility in its sugar and phosphate residues. Although all three ribose moieties display a basically C$^{3'}$-*endo* conformation, their extent of twist differs, as may be gauged from the respective pseudo-rotation angles[19] *P* of 7.0, 15.7 and 27.3°. In contrast to the second nucleotide, whose torsion angle χ [C^4–N^9–C$^{1'}$–O$^{4'}$ − 179.3°] lies in the *anti*-range typical for free purine 5′-nucleotides,[19] both nucleotides 1 and 3 adopt a 'high-*anti*' conformation (χ = −86.9, −90.9°) at the glycosidic bond N^9–C$^{1'}$. A further interesting conformational difference is provided by the *gauche*,

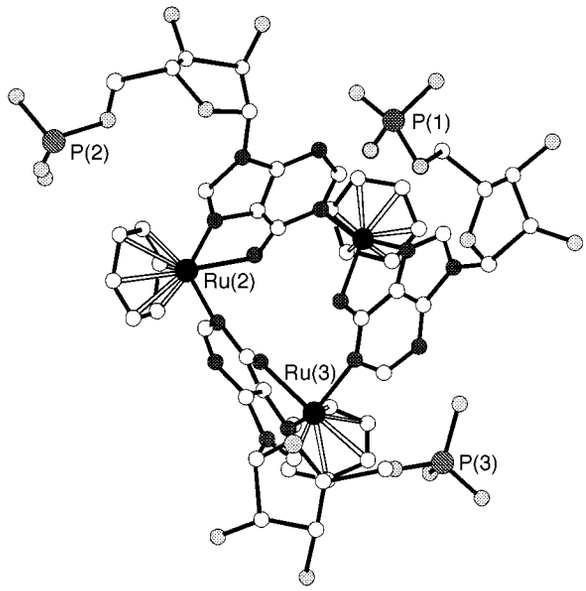

Fig. 2 Molecular structure of [{Ru(5′-AMP)(η⁶-*p*-MeC$_6$H$_4$Pr)}$_3$] **1b** (*p*-cymene substituents have been omitted for clarity)

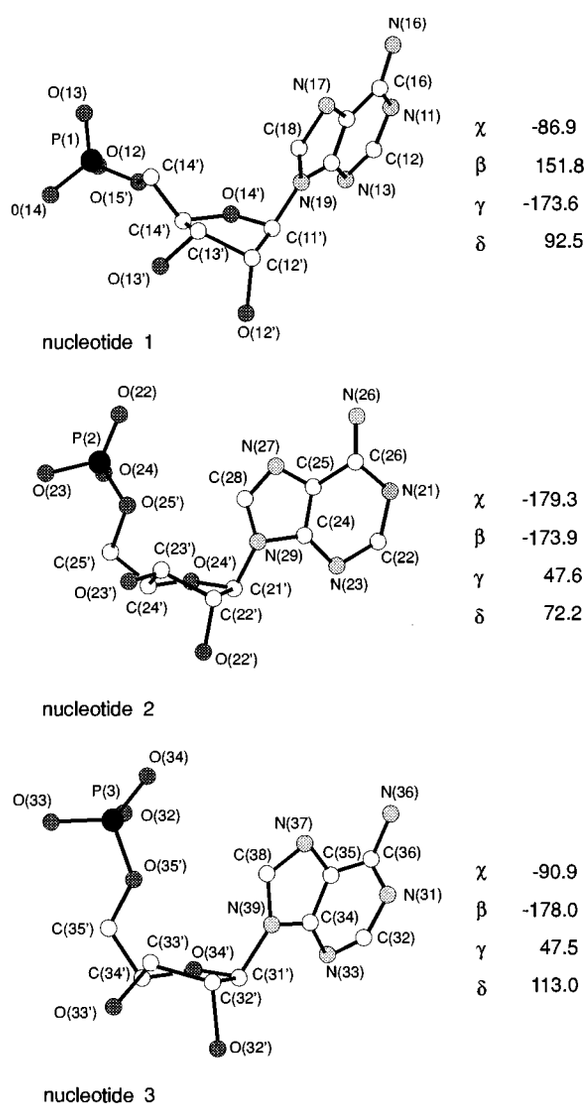

Fig. 3 Conformations of the nucleotide ligands 5′-AMP^{2-} in compound **1b**

trans siting (torsion angles O$^{5'}$–C$^{5'}$–C$^{4'}$–O$^{4'}$, O$^{5'}$–C$^{5'}$–C$^{4'}$–C$^{3'}$ = γ) of the phosphate backbone in nucleotide 1 (torsion angles P–O$^{5'}$–C$^{5'}$–C$^{4'}$ = β, C$^{5'}$–C$^{4'}$–C$^{3'}$–O$^{3'}$ = δ). Both nucleotides 2 and 3 exhibit the *gauche*, *gauche* conformation required for macrochelation. Compound **1b** provides the first example of a purine 5′-nucleotide cyclic oligomer to be structurally characterised by X-ray analysis.

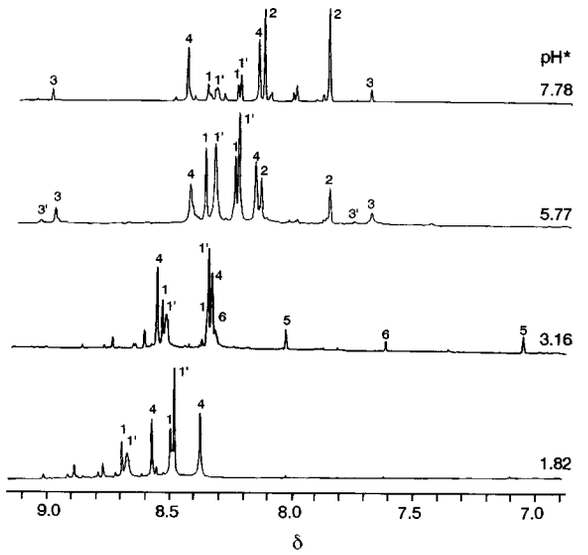

Fig. 4 Selected pH*-dependent ^{1}H NMR spectra for the aqueous equilibrium system 5′-ATP–(η⁶-C$_6$H$_6$)Ru^{II} at the molar ratio $R_{5'\text{-ATP:Ru}}$ = 1.0 (c_{Ru} = 0.050 mol l^{-1}). The signal assignment is as follows: 1,1′, macrochelate [Ru{5′-H$_2$ATP-κ^3*N*^{7},*O*(*P*$_\beta$),*O*(*P*$_\gamma$)}(η⁶-C$_6$H$_6$)] (pH* 3.16); 2, κ*N*^{1} co-ordinated species; 3,3′, cyclic trimers [{Ru(5′-H$_2$ATP)(η⁶-C$_6$H$_6$)}$_3$] (pH* 7.78); 4,5′-H$_2$ATP^{2-}; signals 5 and 6 could not be assigned unequivocally

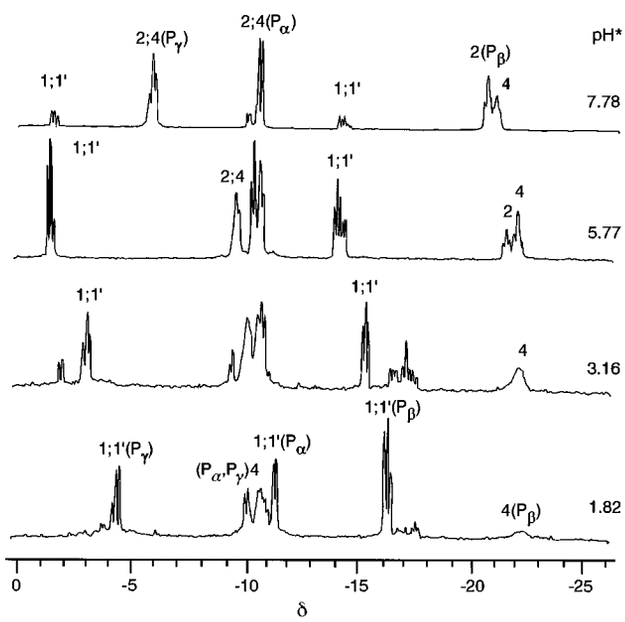

Fig. 5 Selected pH*-dependent ^{31}P-{^{1}H} NMR spectra for the aqueous equilibrium system 5′-ATP–(η⁶-C$_6$H$_6$)Ru^{II} at the molar ratio $R_{5'\text{-ATP:Ru}}$ = 1.0 (c_{Ru} = 0.050 mol l^{-1}). The signal assignment is as for Fig. 4

The interaction of [Ru(η⁶-C$_6$H$_6$)]$^{2+}$ (aq) with adenosine 5′-triphosphate at a molar ratio $R_{5'\text{-ATP:Ru}}$ of 1.0 was investigated by ^{1}H and ^{31}P-{^{1}H} NMR spectroscopy at pH* values in the range 1.82–7.82. Selected NMR spectra are presented in Figs. 4 and 5. The pronounced downfield shift for H^8 accompanied by an upfield shift for H^2 allows an unequivocal assignment of the signal pair 3,3′ to μ-1κ*N*^{1}:2κ^2*N*^{6},*N*^{7} co-ordinated cyclic trimers of the type [{Ru(5′-H$_2$ATP)(η⁶-C$_6$H$_6$)}$_3$] at pH* values of 5.77 and higher. In striking contrast to the analogous 5′-AMP–(η⁶-C$_6$H$_6$)Ru^{II} equilibrium system, this diastereomeric pair (Ru$_S$Ru$_S$Ru$_S$, Ru$_R$Ru$_R$Ru$_R$) cannot be observed in more strongly acid solution (pH* ≤ 3.16) and remains a relatively minor species even at neutral or higher pH* values. Com-

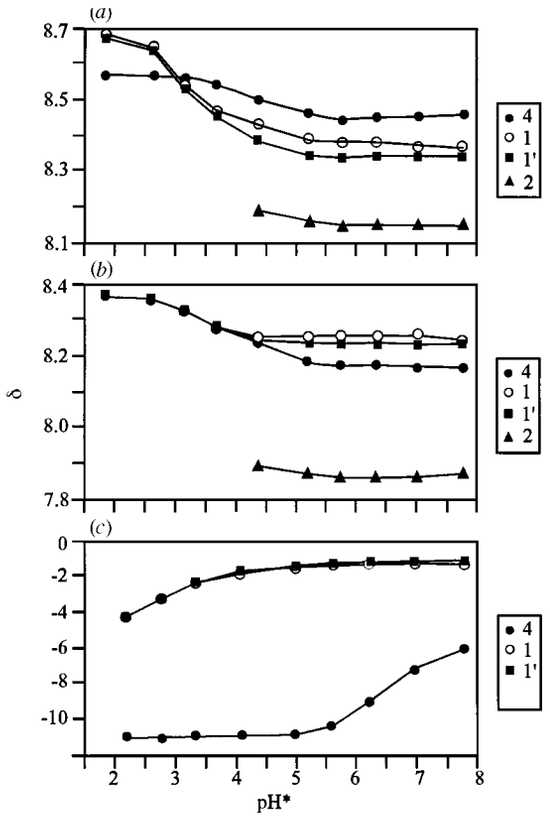

Fig. 6 Chemical shifts of the (*a*) H^8, (*b*) H^2 and (*c*) phosphate P_γ NMR resonances as a function of pH* for the 5′-ATP–(η^6-C_6H_6)Ru^{II} equilibrium system. The signal assignment is as for Fig. 4

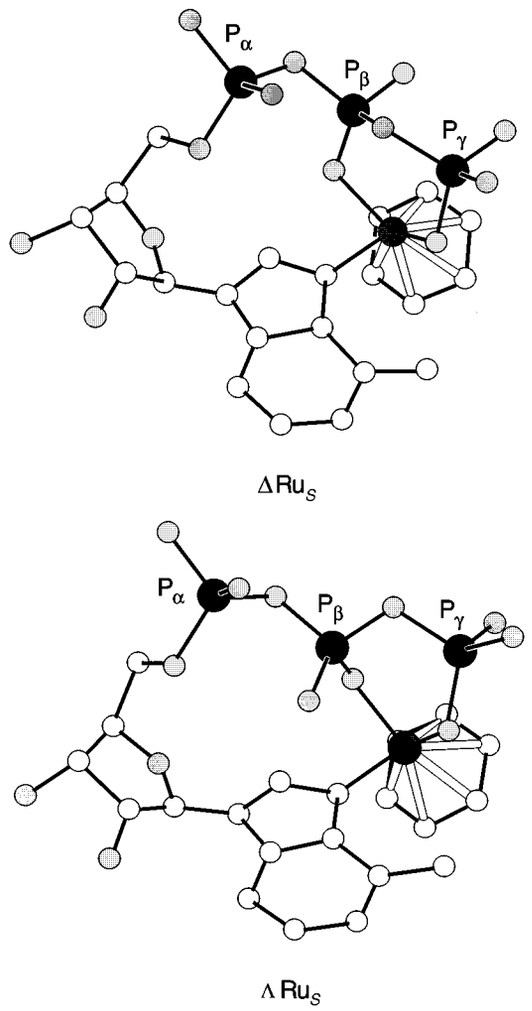

Fig. 7 Structural models for $\kappa^3N^7,O(P_\beta),O(P_\gamma)$ co-ordinated ΔRu_S and ΛRu_S diastereomers

parison of the ^1H and ^{31}P-{^1H} NMR spectra presented in Figs. 4 and 5 indicates that resonances 1,1′ may be assigned to $\kappa^3N^7,O(P_\beta)$, $O(P_\gamma)$ co-ordinated complexes, signals 4 to free adenosine 5′-triphosphate. As may be followed in Fig. 6(*a*) and 6(*b*), the base protons of this nucleotide experience a characteristic shift to higher field in the range pH* 2–6 [pH* 1.82, δ 8.37 (H^2), 8.56 (H^8); pH* 5.77, δ 8.17 (H^2), 8.45 (H^8)] corresponding to deprotonation of the pyrimidine nitrogen N^1 ($pK_a = 3.9$[20]). The pH dependence of the analogous H^2 and H^8 resonances for the species 1,1′ provides clear evidence for an N^7 co-ordination. Not only is the upfield shift more pronounced for these metal complexes, it also takes place in a solution more acid by *ca.* one pH unit [pH* 1.82, δ 8.47, 8.47 (H^2), 8.6, 8.69 (H^8); pH* 5.21, δ 8.25, 8.26 (H^2), 8.35, 8.39 (H^8)]. An enhancement of N^1 deprotonation by up to two pK_s units is typical for N^7 co-ordinated adenine derivatives[15,21] and has also been reported for $N^7/O(P_\alpha)$ macrochelation of the $(Cp)_2Mo^{IV}$ fragment.[9b]

The pronounced low-field shifts of respectively up to 7.8 and 8.6 ppm for the β- and γ-phosphorus atoms of species 1,1′ in the range pH* 1.82–7.78 depicted in Fig. 5 are characteristic for metal–phosphate binding.[7–9] Confirmation of the presence of a β-, α-phosphate six-membered ring in 1,1′ is provided by a P–P COSY (correlation spectroscopy) spectrum recorded at pH* 6.7. The low-field γ-phosphorus atoms at δ −1.19 and −1.04 are found to couple only with the low-field β-phosphorus atoms at δ −14.13 and −13.88. Within the pH* range investigated, the resonances for the non-co-ordinated α-phosphorus atoms of complexes 1,1′ experience only a gradual shift from δ −11.06 (pH* 2.61) to −9.65 (pH* 7.78) and lie close to those of other species and the free nucleoside 5′-triphosphate. As may be followed in Fig. 6(*c*), metal co-ordination of the γ-phosphate group in 1,1′ leads to a marked enhancement of the second deprotonation at this position as evidenced by the earlier low-field shift of the γ-phosphorus resonance in comparison to adenosine 5′-triphosphate itself (signal 4). An analogous reduction in the second pK_s value has been described for $N^7/O(P_\alpha)$ and $N^7/O(P_\gamma)$ macrochelates.[7b,c,9]

The above ^1H and ^{31}P-{^1H} NMR pH-dependent titrations and, in particular, the absence of α-phosphate co-ordination for the equimolar equilibrium systems 5′-AMP–(η^6-C_6H_6)Ru^{II}, 5′-ADP–(η^6-C_6H_6)Ru^{II} (see below) and 5′-ATP–(η^6-C_6H_6)Ru^{II} provide very strong evidence for $\kappa^3N^7,O(P_\beta),O(P_\gamma)$ macrochelation in complexes 1,1′. Both the ruthenium and β-phosphorus atoms are chiral in such macrochelates, meaning that four diastereomers (Figs. 7, 8) are possible, of which at least two give rise to the separate ^1H and ^{31}P-{^1H} NMR resonances at pH* > 4.38. The appearance of additional signals in the H^2/H^8 region of 1,1′ indicates that the presence of further diastereomers cannot be ruled out at lower pH values. As may be seen in Figs. 7 and 8, the adoption of opposing Ru_S or Ru_R chiralities requires strikingly different *anti* or *syn* conformations at the glycosidic bond N^9–$C^{1'}$. The $C^{5'}$–$O^{5'}$ nucleoside bond exhibits a *gauche*, *gauche* orientation for the *S*-configurated metal centre in contrast to the *trans*, *gauche* orientation found in the ΔRu_R and ΛRu_R diastereomers. As the *anti* conformation is typically observed for metal complexes of purine 5′-nucleotides,[2,22] it is possible that species 1,1′ will be the ΔRu_S and ΛRu_S isomers depicted in Fig. 7.

The NMR signals for complex 2 in the 5′-ATP–(η^6-C_6H_6)Ru^{II} equilibrium system are only found at pH* > 4.38, *i.e.* at values for which the pyrimidine nitrogen N^1 (pK_a 3.9) is deprotonated in adenosine 5′-triphosphate. The pronounced high-field shift of its H^2/H^8 resonances [pH* 4.38, δ 8.18 (H^8), 7.90 (H^2); pH* 7.78, δ 8.15 (H^8), 7.87 (H^2)] in comparison to the macrochelates 1,1′ and the rapid increase in its concentration at

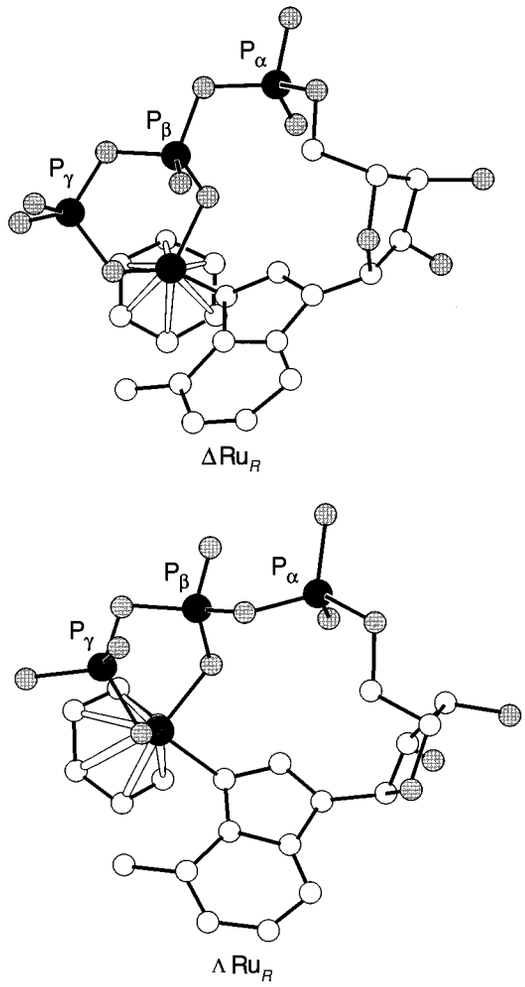

Fig. 8 Structural models for $\kappa^3N^7,O(P_\beta),O(P_\gamma)$ co-ordinated ΔRu_R and ΛRu_R diastereomers

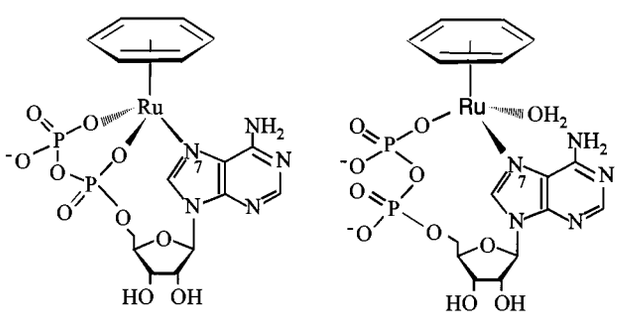

Scheme 3 Possible $\kappa^3N^7,O(P_\alpha),O(P_\beta)$ and $\kappa^2N^7,O(P_\beta)$ macrochelates in the aqueous 5′-ADP–(η^6-C_6H_6)Ru^{II} system

higher pH values both indicate that species 2 must correspond to a κN^1 co-ordinated complex. As the chemical shifts of its α-, β- and γ-phosphorus atoms are recorded at ppm values similar to those of free adenosine 5′-triphosphate, an inner-sphere phosphate co-ordination can be ruled out. The observation[23] of very similar H^2/H^8 resonance positions for [{Rh(η^5-C_5Me_5)-(μ-OH)(9-mhpx-κN^1)}$_2$] (9-Hmhpx = 9-methylhypoxanthine) suggests that the signals 2 in the 5′-ATP–(η^6-C_6H_6)Ru^{II} equilibrium system will correspond to an analogous hydroxo-bridged dimeric complex [{Ru(η^6-C_6H_6)(μ-OH)(5′-H_2ATP-κN^1)}$_2$]$^{2-}$. Signals 5 and 6, of which the latter belongs to a 1:2 species (pH 3.16), could not be assigned with certainty.

Two inner-sphere macrochelates with respectively κ^3N^7, $O(P_\alpha)$, $O(P_\beta)$ and κ^2N^7, $O(P_\beta)$ co-ordination can be postulated for the reaction of adenosine 5′-diphosphate with the (η^6-C_6H_6)Ru^{II} fragment (Scheme 3). In fact, an equimolar reaction solution 5′-ADP–(η^6-C_6H_6)Ru^{II} in the range pH* 2.65–5.92 is

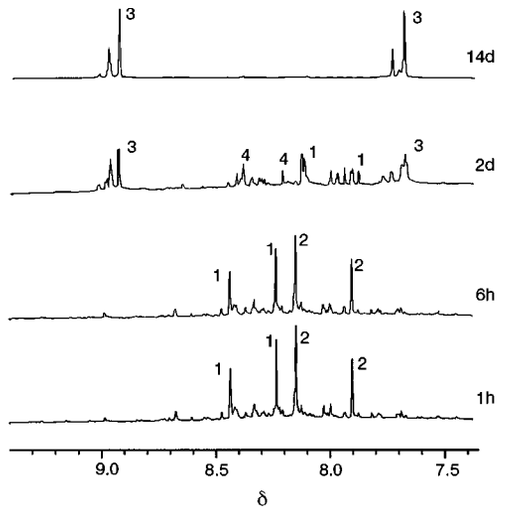

Fig. 9 Time dependence of the ^{1}H NMR spectrum of the 1:1 5′-ADP–(η^6-C_6H_6)Ru^{II} system at pH* 5.61 (c = 0.050 mol l^{-1})

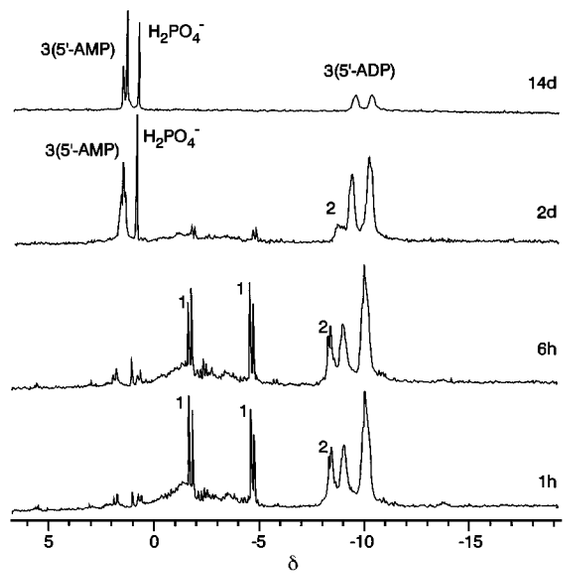

Fig. 10 Time dependence of the ^{31}P{^{1}H} NMR spectrum of the 1:1 5′-ADP–(η^6-C_6H_6)Ru^{II} system at pH* 5.61 (c = 0.050 mol l^{-1})

found to contain a complex 1 the ^{1}H and ^{31}P-{^{1}H} NMR chemical shifts (Figs. 9 and 10) of which are in accordance with the former formulation. For instance its α- and β-phosphorus resonances are shifted by respectively *ca.* 5.5 and 8.5 ppm to lower field in comparison to the free nucleotide. However the remaining ^{31}P-{^{1}H} NMR signals are rather broad and a time-dependent study demonstrates that $O(P_\alpha)$, $O(P_\beta)$ co-ordination is presumably followed by cleavage of the terminal phosphate group.

The dramatic change in the appearance of the ^{1}H and ^{31}P-{^{1}H} NMR spectra of the 5′-ADP–(η^6-C_6H_6)Ru^{II} reaction system (initial pH* 5.61) over a period of 14 d is illustrated by the selected spectra presented in Figs. 9 and 10. Two major species 1 and 2 are present in the reaction solution after 1 h. As was discussed for the 5′-ATP–(η^6-C_6H_6)Ru^{II} system, the high-field resonances 2 may be assigned to an N^1-co-ordinated complex without phosphate binding. An apparently metal-assisted phosphate cleavage then leads to total disappearance of both 1 and 2 within 14 d and the exclusive formation of a variety of μ-1κN^1:2κ^2N^6, N^7 co-ordinated cyclic trimers 3 with their typical pronounced opposite H^2 and H^8 chemical shifts (*ca.* 7.7, 9.0 ppm). The occurrence of more than two ^{1}H resonances for each of these adenine protons and the observation of low-intensity α- and β-phosphorus signals in the ^{31}P-{^{1}H} NMR spectrum

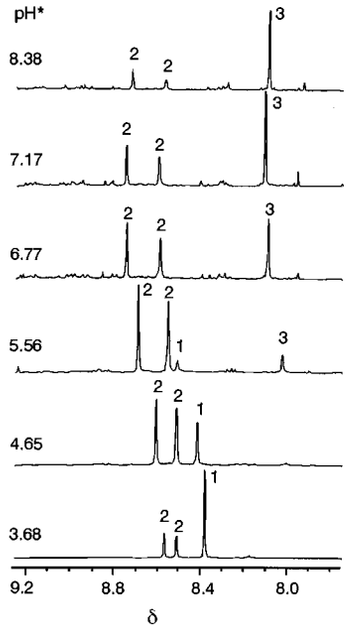

Fig. 11 Selected pH*-dependent ^{1}H NMR spectra for the aqueous equilibrium system 5′-GMP–(η^6-C_6H_6)Ru^{II} at the molar ratio $R_{5'\text{-GMP:Ru}} = 1.0$ ($c_{Ru} = 0.050$ mol l^{-1}). The signal assignment at pH* 5.56 is as follows: 1, [Ru(5′-HGMP)(η^6-C_6H_6)$(D_2O)_2$]$^+$; 2, [Ru(5′-HGMP)$_2$(η^6-C_6H_6)(D_2O)]; 3, 5′-$HGMP^-$

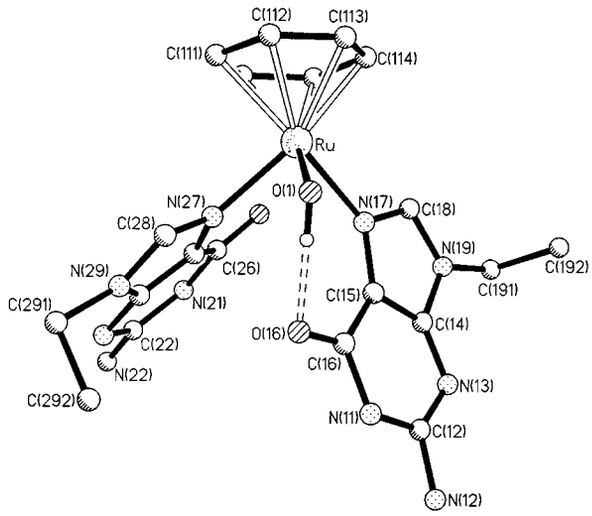

Fig. 12 Molecular structure of the cation of [Ru(η^6-C_6H_6)(9-egua)$_2$-(H_2O)][CF_3SO_3]$_2$ **2**. Protons have been omitted for clarity

after 14 d indicates the presence of mixed 5′-AMP–5′-ADP cyclic trimers. Free $H_2PO_4^-$ provides the ^{31}P-{^{1}H} NMR singlet at *ca.* δ 1.1.

The promotion of phosphate cleavage by κ^2N^7, $O(P)$ macrochelation has been reported for other metals.[24] In contrast to adenosine 5′-diphosphate, a time-dependent study of the 5′-ATP–(η^6-C_6H_6)Ru^{II} reaction system offers no evidence for significant hydrolysis of the pyrophosphate residue over a similar period of time. This finding suggests that the marked reduction in strain for κ^3N^7, $O(P_\beta)$, $O(P_\gamma)$ in comparison to κ^3N^7, $O(P_\alpha)$, $O(P_\beta)$ co-ordination will lead to an increased thermodynamic and/or kinetic stability of adenosine 5′-triphosphate macrochelates with respect to phosphate cleavage and reorganisation to μ-1κN^1:2κ^2N^6, N^7 cyclic trimers.

Guanosine 5′-nucleotides

In striking contrast to the co-ordination behaviour of 5′-AMP^{2-}, reaction of [Ru(η^6-C_6H_6)$(D_2O)_3$]$^{2+}$ with guanosine 5′-monophosphate leads solely to the formation of κN^7-co-ordinated 1:1 (1) and 2:1 (2) complexes in the range pH* 3.69–8.38 (Fig. 11). As cyclic trimer formation with μ-1κN^1:2κN^7,O^6 bridging has been reported[23] for the 9-ethylhypoxanthine–(η^5-C_5Me_5)Rh^{III} equilibrium system, it seems reasonable to assume that the steric requirements of the guanine 2-amino substituent adjacent to the required binding site N^1 will prevent an analogous co-ordination mode for 5′-GMP^{2-}.

In comparison to the free 5′-nucleotide (signal 3), the H^8 protons in species 1 and 2 exhibit a low-field shift [pH* 5.56 δ 8.50 (1); 8.55, 8.67 (2); 8.02 (3)] in a range 0.48–0.65 ppm characteristic for N^7 co-ordination. The 2:1 complex [Ru-(5′-HGMP)$_2$(η^6-C_6H_6)(D_2O)] (2) dominates for pH* values above 4.65. Absence of phosphate co-ordination is confirmed by the registration of ^{31}P-{^{1}H} resonances at chemical shift values typical for the free nucleotide (pH* 3.69, δ 0.77 (1); 1.03, 1.28 (2); pH* 8.38, δ 4.55, 4.71 (2); 4.13 (3)]. Loss of the second phosphate proton with its pK_a value of *ca.* 6 generates a characteristic shift of both the H^8 and α-phosphorus resonances to lower field over the range pH* 4.5–7.5. Model complex **2**, prepared by reaction of [{$RuCl_2$(η^6-C_6H_6)}$_2$] with 9-ethylguanine (9-egua) in methanol after addition of 2 equivalents of Ag-(O_3SCF_3), exhibits a co-ordination pattern similar to that of species 2 in the 5′-GMP–(η^6-C_6H_6)Ru^{II} equilibrium system. Atom N^7 is bonded to ruthenium as has also been reported for *cis*-[RuCl(bipy)$_2$(9-egua)]Cl (bipy = 2,2′-bipyridine).[25] As depicted in Fig. 12, the oxo atom O(16) of one of the egua ligands of **2** participates in an outer-sphere fashion in the pseudo-tetrahedral co-ordination sphere of the ruthenium atom Ru(1), through a relatively strong O···H–O hydrogen bond of length 2.537 Å between O(16) and the co-ordinated water molecule. Despite the differing binding modes of the two egua ligands, complex **2** exhibits only one H^8 resonance at δ 8.57, in contrast to species 2 of the 5′-GMP–(η^6-C_6H_6)Ru^{II} system which generates two H^8 singlets of equal intensity. Outer-sphere macrochelation involving a (P)O···H–O interaction for one of the 5′-GMP ligands may well be responsible for this observation and supporting evidence for this suggestion is provided by the presence of two ^{31}P-{^{1}H} resonances for the α-phosphorus atom of 2.

Analogous κN^7 co-ordinated 1:1 and 2:1 complexes 1 and 2 are also present at lower pH* values in the 5′-GTP–(η^6-C_6H_6)Ru^{II} equilibrium system, for which selected pH*-dependent ^{1}H and ^{31}P-{^{1}H} NMR spectra are presented in Figs. 13 and 14. However, as for adenosine 5′-triphosphate, the introduction of two additional phosphate groups leads to the competitive formation of κ^3N^7, $O(P_\beta)$, $O(P_\gamma)$ macrochelates (3,3′), which suppress species 1 and 2 at pH* values above 5.75. In contrast, the 2:1 species is present as the major complex for the 5′-GMP–(η^6-C_6H_6)Ru^{II} system in the range pH* 5.56–8.38 (Fig. 11). Signal 4, in Figs. 13 and 14, belongs to free guanosine 5′-triphosphate, signal 5 to a 1:2 complex that could not be assigned unambiguously. Two further uncharacterised species are represented by signals 6 and 7 at pH* values of 3.30 and 4.73.

Typical ^{31}P-{^{1}H} NMR shifts of respectively *ca.* 6.6 and 6.0 ppm to lower field are exhibited by the β- and γ-phosphorus atoms of guanosine 5′-triphosphate in the macrochelates 3,3′. The P–P COSY spectra at pH* values of 5.25 and 6.31 confirm that P_β, P_γ coupling is solely between co-ordinated phosphate groups. No evidence was found for the presence of κ^2N^7, $O(P_\beta)$ or κ^2N^7, $O(P_\gamma)$ macrochelates. As illustrated by the characteristic low-field shift for the γ-phosphorus resonance, ruthenium co-ordination of the terminal phosphate group in 3,3′ leads to a reduction in the pK_a value by about 2 units for the second deprotonation at this position. The H^8 resonances of the macrochelates 3,3′ (pH* 5.35, δ 7.72, 7.86) are shifted to higher field with respect to the free nucleotide 5′-triphosphate (pH* 5.35, δ 8.04). This observation is, at first sight, somewhat surprising, in view of the fact that the κN^7-co-ordinated complexes 1 and 2 display a pronounced low-field shift [pH* 5.35, δ 8.41 (1), 8.49,

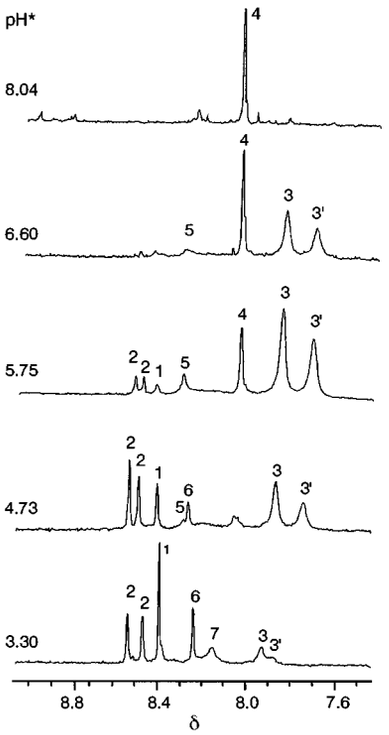

Fig. 13 Selected pH*-dependent ^{1}H NMR spectra for the aqueous equilibrium system 5′-GTP–(η^{6}-C_6H_6)Ru^{II} at the molar ratio $R_{5'\text{-GTP:Ru}} = 1.0$ ($c_{Ru} = 0.040$ mol l^{-1}). The signal assignment is as follows: 1, [Ru(5′-H_3GTP)(C_6H_6)(D_2O)$_2$]$^{+}$ (pH* 3.30); 2, [Ru(5′-H_3GTP)$_2$(C_6H_6)(D_2O)] (pH* 3.30); 3, [Ru{5′-HGTP-κ$^{2}N^{7}$,$O(P_\beta)$,-$O(P_\gamma)$}(η^{6}-C_6H_6)]$^{-}$ (pH* 5.75); 4, 5′ H_2GTP^{2-}. Signals 5–7 cold not be characterised unambiguously

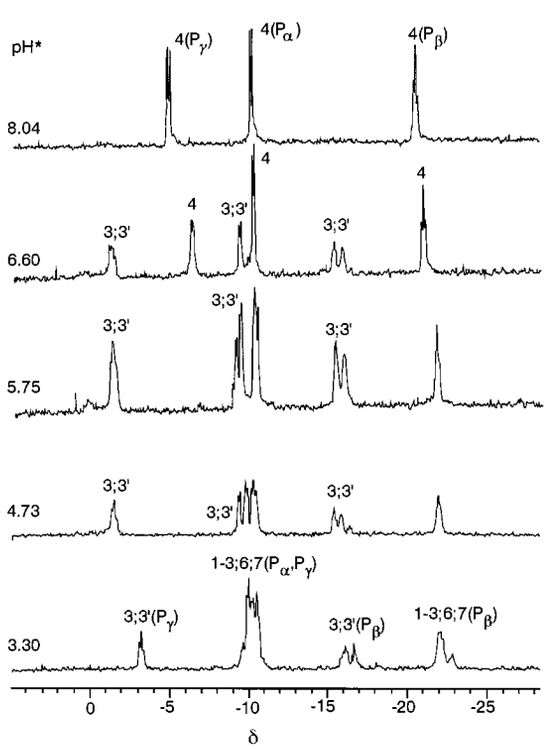

Fig. 14 Selected pH*-dependent ^{31}P-{^{1}H} NMR spectra for the aqueous equilibrium system 5′-GTP–(η^{6}-C_6H_6)Ru^{II} at the molar ratio $R_{5'\text{-GTP:Ru}} = 1.0$ ($c_{Ru} = 0.040$ mol l^{-1}). Signal assignment is as for Fig. 13

8.52 (2)]. However, the κ$^{2}N^{7}$, $O(P_\alpha)$ macrochelate formed by the reaction of the $(cp)_2Mo^{IV}$ fragment with 5′-dGMP^{2-} is known to exhibit an H^{8} resonance with a chemical shift[9] similar to that of 3,3′.

Furthermore, the known preference of guanine derivatives for N^{7} co-ordination in acid or neutral solution and the disappearance of signals for 3,3′ in alkaline solution all indicate binding to the imidazole ring. Additional support for this assignment is provided by the broadness of the proton resonances for 3 and 3′, which would be expected if more than two diastereomers are present in solution and/or if the sugar and triphosphate residues were to exhibit pronounced conformational flexibility. Inspection of Figs. 7 and 8 for the macrochelates of adenosine 5′-triphosphate indicates that the C^{8}–H^{8} bond must point towards the phosphate backbone in the κ$^{3}N^{7}$, $O(P_\beta)$, $O(P_\gamma)$ co-ordination mode. This may provide an explanation for the increased extent of shielding experienced by H^{8} in the species 3,3′ of the 5′-GTP–(η^{6}-C_6H_6)Ru^{II} equilibrium system.

No evidence for a significant extent of metal-assisted cleavage of the pyrophosphate backbone in guanosine 5′-triphosphate could be obtained from a time-dependent NMR investigation. This behaviour is once again in striking contrast to that of the nucleoside 5′-diphosphate. The ^{31}P-{^{1}H} NMR spectra at pH* 5.04 for the 5′-GDP–(η^{6}-C_6H_6)Ru^{II} system after 1 h contains both a broad resonance (δ 0.1) for the β-phosphorus atoms of κ$^{2}N^{7}$, $O(P_\beta)$-co-ordinated macrochelates and a number of adjacent (δ 0.8–2.2) sharp signals belonging to κN^{7}-co-ordinated 5′-monophosphate complexes and free 5′-HGMP^{-} and $H_2PO_4^{-}$. Phosphate cleavage proceeds more rapidly than for adenosine 5′-diphosphate. Although the number and the broadness of the NMR signals prevent a detailed analysis of the system it is possible to assign the macrochelate resonances without difficulty. A low-field shift for the β-phosphorus atom of *ca.* 8 ppm provides confirmation of phosphate co-ordination. In contrast to the macrochelates of the 5′-GTP–(η^{6}-C_6H_6)Ru^{II} equilibrium system, the H^{8} resonance is shifted by *ca.* 0.2 ppm to lower field, a value more typical for N^{7} co-ordination.

The present study provides the first systematic analysis of competition between macrochelation and oligomer formation for purine 5′-nucleotides. In fact, macrochelates are only formed with the (η^{6}-C_6H_6)Ru^{II} fragment by nucleoside 5′-di- and -tri-phosphates and, in the former case, facilitate a slow metal-assisted phosphate cleavage. Steric requirements of the 2-amino substituent in guanosine 5′-monophosphate prevent the formation of cyclic trimers, which, in contrast, are predominant for the analogous adenine nucleotide. This restricts the palette of 5′-GMP complexes to 1:1 and 2:1 κN^{7} co-ordinated species.

The organometallic moiety (η^{6}-C_6H_6)Ru^{II} has been shown to provide a stable facially tridentate half-sandwich fragment well suitable for analytical bioco-ordination chemistry in aqueous solution.

Experimental

Solvents were dried and distilled before use. Proton and ^{31}P NMR spectra were recorded on a Bruker AM-400 spectrometer, FAB mass spectra on a Fisons VG Autospec instrument using 3-nitrobenzyl alcohol as the matrix. Elemental analyses were performed on a Carlo Erba 1106 analyser. The starting materials [{$RuCl_2$(η^{6}-C_6H_6)}$_2$] and [{$RuCl_2$(η^{6}-*p*-$MeC_6H_4Pr^{i}$)}$_2$] were prepared according to literature procedures.[26,27] The purine 5′-nucleotides were obtained from Sigma and used as received.

Syntheses

[{Ru(5′-HAMP)(η^{6}-*p*-$MeC_6H_4Pr^{i}$)}$_3$][CF_3SO_3]$_3$ 1a. The compound $Ag(O_3SCF_3)$ (0.167 g, 0.653 mmol) was added to a solution of [{$RuCl_2$(η^{6}-*p*-$MeC_6H_4Pr^{i}$)}$_2$] (0.100 g, 0.163 mmol) in acetone (5 cm^{3}). After removal of AgCl by filtration, 5′-H_2AMP (0.145 g, 0.327 mmol) was added to the filtrate and the resulting suspension stirred for 3 d at room temperature to afford compound **1** as an orange precipitate in 56% yield (0.120

g) (Found: C, 35.5; H, 4.5; N, 10.0. $C_{63}H_{81}F_9N_{15}O_{30}P_3Ru_3S_3$ requires C, 34.5; H, 3.7; N, 9.6%). FAB mass spectrum: *m/z* 1892 (1, $[M - 2CF_3SO_3]^+$), 1397 (1, $[M - 5'\text{-HAMP} - 3CF_3SO_3]^+$), 1162 {1, $[M - Ru(\eta^6\text{-}p\text{-}MeC_6H_4Pr^i) - 5'\text{-HAMP} - 3CF_3SO_3]^+$} and 370 {100%, $[Ru(HAde)(\eta^6\text{-}p\text{-}MeC_6H_4Pr^i)]^+$}. ^{1}H NMR ($D_2O$): δ (selected) 7.67, 7.72 (2s, H^2 of **1**), 8.33 (s, H^2 of 5′-AMP^{2-}), 8.50 (s, H^8 of 5′-AMP^{2-}), 9.00, 9.01 (2s, H^8 of **1**). Suitable crystals of $[\{Ru(5'\text{-AMP})(\eta^6\text{-}p\text{-}MeC_6H_4Pr^i)\}_3]$. 7.5 H_2O **1b** for an X-ray structural analysis were grown by slow evaporation of an aqueous solution of **1a**.

$[Ru(\eta^6\text{-}C_6H_6)(9\text{-egua})_2(H_2O)][CF_3SO_3]_2$ 2. The compound $Ag(O_3SCF_3)$ (0.204 g, 0.8 mmol) was added to a suspension of $[\{RuCl_2(\eta^6\text{-}C_6H_6)\}_2]$ (0.100 g, 0.2 mmol) in MeOH (5 cm^3). After removal of the resulting AgCl by filtration, 9-ethylguanine (0.143 g, 0.8 mmol) was added to the filtrate, which was stirred for 2 d. The resulting precipitate was filtered off and recrystallised from an MeOH–water–Et_2O solution at −30 °C to afford crystals of compound **2** in 68% yield (Found: C, 30.0; H, 3.6; N, 16.3. $C_{22}H_{26}F_6N_{10}O_9RuS_2\cdot 2H_2O$ requires C, 29.7; H, 3.4; N, 15.7%). FAB mass spectrum: *m/z* 687 (1, $[M - CF_3SO_3 - H_2O]^+$), 537 (96, $[M - 2CF_3SO_3 - H_2O]^+$) and 358 (100%, $[M - 2CF_3SO_3 - 9\text{-egua} - H_2O]^+$). ^{1}H NMR [$D_2O$–$(CD_3)_2$-CO]: δ 1.37 (6 H, t, CH_3), 3.5 (2 H, s, H_2O), 4.12 (4 H, q, CH_2), 6.21 (6 H, s, C_6H_6) and 8.57 (2 H, s, H^8).

NMR Spectroscopy

The 400 MHz ^{1}H and 162 MHz ^{31}P-{^{1}H} NMR spectra were recorded at 293 K with respectively sodium 3-(trimethylsilyl)tetradeuteriopropionate as internal and 85% H_3PO_4 as external standard. Stock solutions of $[Ru(\eta^6\text{-}C_6H_6)(D_2O)_3]^{2+}$ were prepared by stirring $Ag(O_3SCF_3)$ (0.257 g, 1.0 mmol) with $[\{RuCl_2(\eta^6\text{-}C_6H_6)\}_2]$ (0.126 g, 0.25 mmol) in D_2O (5 cm^3) for 2 h. After removal of precipitated AgCl the volume was increased to 10 cm^3 to provide a solution of concentration 0.050 mol l^{-1}. Solution pH values were measured on a Metrohm 691 pH meter using a Hamilton microcombination electrode (Minitrode 238 100) calibrated with Riedel-de Haen standard buffers (pH 4.00, 7.00). Readings for D_2O solutions were recorded directly prior to NMR measurement in 5 mm tubes. These are designated as pH* values as corrections for deuterium isotope effects were not employed. Reaction solutions were allowed to stand for 2 d at room temperature prior to NMR studies to ensure equilibrium conditions. Adjustment to the required pH* value was achieved by addition of 1.5 mol dm^{-3} NaOD.

X-Ray crystallography

Unit-cell constants were obtained by least-squares refinement on centred angles for 25 reflections ($25 < 2\theta < 30°$) on a Siemens P4 diffractometer. Intensity data were collected at 293 K on the diffractometer in the ω-scan mode with monochromated Mo-Kα radiation (λ = 0.710 73 Å) at 293 K. In each case three control reflections were monitored after collection of 100 reflections; no significant alterations in their intensities were registered. Semiempirical absorption corrections were applied on the basis of ψ-scan data. The structures were solved by a combination of Patterson and Fourier-difference syntheses and refined by full-matrix least squares against F using the SHELXTL set of programs.[28] Scattering factors and corrections for anomalous dispersion were taken from ref. 29; R' is defined as $[\Sigma w(|F_o| - |F_c|)^2/\Sigma w|F_o|^2]^{\frac{1}{2}}$.

Complex 1b. *Crystal data.* $C_{60}H_{78}N_{15}O_{21}P_3Ru_3\cdot 7.5H_2O$, $M = 1876.6$, orthorhombic, space group $P2_12_12_1$ (no. 19), $a = 17.623(4)$, $b = 19.288(4)$, $c = 23.238(5)$ Å, $U = 7899(3)$ $Å^3$, $Z = 4$, $D_c = 1.575$ Mg m^{-3}, $F(000) = 3840$, orange prism with dimensions 0.39 × 0.42 × 0.58 mm, μ(Mo-Kα) = 0.72 mm^{-1}, transmission factors 0.37–0.49, data collection range $4.0 \leqslant 2\theta \leqslant 45.0°$, $+h$, $+k$, $+l$, 5748 independent reflections measured, 3939 with $F_o^2 > 2\sigma(F_o^2)$ were employed in the least-squares refinement.

Structure solution and refinement. Anisotropic thermal parameters were introduced for the Ru, P and, where possible, the nucleotide O, N and C atoms. The high U_{eq} values for some of the atoms of the sugar and phosphate moieties of the second and third 5-AMP^{2-} ligands suggest the presence of static disorder, which could not, however, be successfully modelled. Inclusion of hydrogen atoms at calculated positions did not lead to a significant improvement in the reliability indices and these were, therefore, omitted from the final refinement. The terminal values of R and R' were 0.084 and 0.079 for 731 parameters with weights given by $w = 1/[\sigma^2(F_o)]$; goodness of fit = 1.88, maximum $\Delta/\sigma = 0.056$, maximum, minimum $\Delta\rho$ = 0.84, −0.77 e $Å^{-3}$. The absolute configuration was confirmed by an η refinement to 0.9(2).[30]

Complex 2·2H$_2$O. *Crystal data.* $C_{22}H_{30}F_6N_{10}O_{11}RuS_2$, M = 889.7, monoclinic, space group $C2/c$ (no. 15), $a = 25.218(5)$, $b = 24.264(5)$, $c = 12.811(3)$ Å, $U = 6971(3)$ $Å^3$, $Z = 8$, D_c = 1.692 Mg m^{-3}, $F(000) = 3584$, yellow prism with dimensions 0.15 × 0.18 × 0.43 mm, μ(Mo-Kα) = 0.67 mm^{-1}, transmission factors 0.80–0.87, data collection range $3.0 \leqslant 2\theta \leqslant 45.0°$, $+h$, $+k$, $+l$; 4774 reflections measured of which 4520 ($R_{int} = 0.018$) were unique. 1920 Reflections with $F_o^2 > 2\sigma(F_o^2)$ were employed in the least-squares refinement.

Structure solution and refinement. One of the $CF_3SO_3^-$ anions is disordered with its two possible S atom positions lying on a crystallographic C_2 axis; the atoms O(21)–F(23) and O(21′)–F(23′) of the disordered anion exhibit site occupation factors of 0.5. The high group isotropic thermal parameters for these atoms (0.132–0.266 $Å^3$) suggest a degree of secondary disorder, that could not be modelled in a satisfactory manner. Anisotropic thermal parameters were introduced for the non-hydrogen atoms of the cation, the S atoms of $CF_3SO_3^-$ and the water O atoms. Inclusion of calculated hydrogen-atom positions in the final least-squares refinement cycles did not lead to an improvement in R and R' and on this ground these atoms were not considered. The final values of R and R' were 0.095 and 0.100 for 409 parameters with weights given by $w^{-1} = \sigma^2(F_o) + 0.0008F_o^2$; goodness of fit = 1.87, maximum Δ/σ = 0.033, maximum, minimum $\Delta\rho$ = 1.27, −0.71 e $Å^{-3}$ with the highest peaks in the region of the disordered $CF_3SO_3^-$ anions. The high values of R and R' reflect the failure fully to describe the $CF_3SO_3^-$ disorder.

Atomic coordinates, thermal parameters, and bond lengths and angles have been deposited at the Cambridge Crystallographic Data Centre (CCDC). See Instructions for Authors, *J. Chem. Soc., Dalton Trans.*, 1997, Issue 1. Any request to the CCDC for this material should quote the full literature citation and the reference number 186/479.

References

1 H. Lönnberg, in *Biocoordination Chemistry*, ed. K. Bürger, Ellis Horwood, Chichester, 1990, p. 284.
2 A. Terrón, *Comments Inorg. Chem.*, 1993, **14**, 63.
3 H. Sigel, *Chem. Soc. Rev.*, 1993, 255.
4 H. Sigel, S. S. Massoud and N. A. Corfu, *J. Am. Chem. Soc.*, 1994, **116**, 2958.
5 S. E. Sherman and S. J. Lippard, *Chem. Rev.*, 1987, **87**, 1153.
6 A. Szent-Györgyi, in *Enzymes: Units of Biological, Structure and Function*, ed. O. H. Gaebler, Academic Press, New York, 1956, p. 393.
7 (*a*) M. D. Reily and L. G. Marzilli, *J. Am. Chem. Soc.*, 1986, **108**, 8299; (*b*) M. D. Reily, T. W. Hambley and L. G. Marzilli, *J. Am. Chem. Soc.*, 1988, **110**, 2999; (*c*) E. Alessio, Y. Xu, S. Cauci, G. Mestroni, G. Quadrifoglio, P. Viglino and L. G. Marzilli, *J. Am. Chem. Soc.*, 1989, **111**, 7068; (*d*) L. M. Torres and L. G. Marzilli, *J. Am. Chem. Soc.*, 1991, **113**, 4678.

8 M. Green and J. M. Miller, *J. Chem. Soc., Chem. Commun.*, 1987, 1864 (correction 1988, 404); D. J. Evans, M. Green and R. van Eldik, *Inorg. Chim. Acta*, 1987, **128**, 27; D. M. Orton and M. J. Green, *J. Chem. Soc., Chem. Commun.*, 1991, 1612.
9 (*a*) L. Y. Kuo, M. G. Kanatzidis and T. J. Marks, *J. Am. Chem. Soc.*, 1987, **109**, 7207; (*b*) L. Y. Kuo, M. G. Kanatzidis, M. Sabat, A. L. Tipton and T. J. Marks, *J. Am. Chem. Soc.*, 1991, **113**, 9027.
10 H. Sigel, S. S. Massoud and R. Tribolet, *J. Am. Chem. Soc.*, 1988, **110**, 6857.
11 R. S. Taylor and H. Diebler, *Bioinorg. Chem.*, 1976, **6**, 247; A. Peguy and H. Diebler, *J. Phys. Chem.*, 1977, **81**, 1355; H. Diebler, *J. Mol. Catal.*, 1984, **23**, 209.
12 H. Sigel and K. H. Scheller, *Eur. J. Biochem.*, 1984, **138**, 291.
13 (*a*) U. K. Häring and R. B. Martin, *Inorg. Chim. Acta*, 1983, **80**, 1; (*b*) K. J. Barnham, C. J. Bauer, M. I. Djuran, M. A. Mazid, T. Rau and P. J. Sadler, *Inorg. Chem.*, 1995, **34**, 2826.
14 K. Uchida, A. Toyama, Y. Tamura, M. Sugimura, F. Mitsumori, Y. Furukawa, H. Takeuchi and I. Harada, *Inorg. Chem.*, 1989, **28**, 2067.
15 K. H. Scheller, V. Scheller-Krattiger and R. B. Martin, *J. Am. Chem. Soc.*, 1981, **103**, 6833.
16 (*a*) W. S. Sheldrick, H. S. Hagen-Eckhard and S. Heeb, *Inorg. Chim. Acta*, 1993, **206**, 15; (*b*) S. Korn and W. S. Sheldrick, *Inorg. Chim. Acta*, 1997, **254**, 85.
17 (*a*) D. P. Smith, E. Baralt, B. Morales, M. M. Olmstead, M. F. Maestre and R. H. Fish, *J. Am. Chem. Soc.*, 1992, **114**, 10 647; (*b*) D. P. Smith, E. Kohen, M. F. Maestre and R. H. Fish, *Inorg. Chem.*, 1993, **32**, 4119; (*c*) H. Chen, M. F. Mastre and R. H. Fish, *J. Am. Chem. Soc.*, 1995, **117**, 3631.
18 M. Stebler-Röthlisberger, W. Hummel, P.-A. Pittet, H.-B. Burgi, A. Ludi and A. E. Merbach, *Inorg. Chem.*, 1988, **27**, 1358.
19 W. Saenger, *Principles of Nucleic Acid Structure*, Springer, New York, 1984.
20 E. Alberica, D. Dewaele, T. Kiss and G. Micera, *J. Chem. Soc., Dalton Trans.*, 1995, **425**.
21 R. B. Martin, *Acc. Chem. Res.*, 1985, **18**, 32.
22 K. Aoki, in *Metal Ions in Biological Systems*, ed. H. Sigel, Marcel Dekker, New York, 1996, vol. 33.
23 H. Chen, M. M. Olmstead, D. P. Smith, M. F. Maestre and R. H. Fish, *Angew. Chem.*, 1995, **107**, 1590.
24 H. Sigel, *Coord. Chem. Rev.*, 1990, **100**, 45.
25 P. M. van Vliet, J. G. Haasnoot and J. Reedijk, *Inorg. Chem.*, 1994, **33**, 1934.
26 R. A. Zelonka and M. C. Baird, *Can. J. Chem.*, 1972, **50**, 3063.
27 M. A. Bennett, T. N. Huang, T. W. Matheson and K. A. Smith, *Inorg. Synth.*, 1982, **21**, 74.
28 G. M. Sheldrick, SHELXTL PLUS programs for use with Siemens X-ray systems, University of Göttingen, 1990.
29 *International Tables for X-Ray Crystallography*, Kynoch Press, Birmingham, 1974, vol. 4.
30 D. Rogers, *Acta Crystallogr., Sect. A*, 1981, **37**, 734.

Received 11*th February* 1997; *Paper* 7/00976C